ON THE USE OF POLARIMETRIC SAR DATA FOR SHIP DETECTION

R. Touzi
Canada Centre for Remote Sensing
588 Booth Street, Ottawa
Ontario, Canada K1A OY7

Abstract— **The polarization information is investigated for ship detection, using the polarimetric Convair-580 SAR. Ocean and ship polarimetric signatures are analysed within the incidence angle range 45°-70° using a data set off the Nova Scotia coast. It is shown that among the classical linear polarizations HH, VV, and HV, the polarization HH gives the best ship-sea contrast at grazing angles, even though the sea clutter is the lowest for the HV polarization. Circular polarizations performs better than the HH polarization at lower incidence angles. The polarization entropy is investigated for use in ship detection. It permits a significant improvement of the ship-sea contrast for incidence angles up to 60°. For larger incidence angles, the increasing heterogeneity of the ocean scattering mechanisms reduces the efficiency of the polarization entropy tool for ship discrimination.**

I. Introduction

Ship detection by synthetic aperture radar (SAR) has become a topic of considerable interest since the upsurge in the commercial market for this type of information. The importance of the transmitting-receiving antenna polarizations on ship detectability is now well recognized. Better ship-sea contrast is obtained with HH whereas VV provides more information on the sea conditions [7], [2]. Radiometric information provided by classical polarization channel (HH, VV, or HV) is not generally sufficient for effective ship detection, and detection methods which are generally based on a thresholding decision over the sea clutter K distribution are also limited. These methods might lead to some identification of ships provided that the ship radar cross section is relatively well distinguished from the random realisation of the K distributed sea clutter.

In this paper, the potential of polarimetric SARs for characterisation of target scattering mechanisms is investigated for ship-sea discrimination. Polarimetric data were collected over a scene with several ships in Nova Scotia (Canada) with the Department of the Environment airborne Convair-580 SAR. During the flight of low wind conditions (7 knots, [3]), reference point targets were deployed. These targets were used to calibrate in magnitude and phase the four measured linear polarizations (HH, VV, HV, and VH), as explained in Section II. The polarimetric signatures of sea and ships are analysed in Section III. Finally, the polarization entropy is investigated for ship discrimination within the 45° -70° incidence angle range of the illuminated scene.

II. Calibration of the polarimeric Convair-580 SAR

In order to exploit the fully polarimetric capability of the Convair-580 SAR, pure H and V polarizations have to be retrieved from the four complex measurements HH, VV, HV, and VH. The general calibration method described in [5] is adapted to calibrate the C-band SAR data described in [4]. In contrast to the X-band system described in [5], the polarizations switches are highly isolated (better than 50 dB). As the H and V antennas are highly isolated (35 dB) and their phase centers are co-located (at least for illumination angles of ±20 degrees from the boresight angle), the system can be calibrated using a corner reflector and a recirculating 45-45 Polarimetric Active Radar Calibrator (PARC) placed at the same illumination angle. The antenna high isolation, and the knowledge of the H and V antenna gain patterns permit to extend the calibration in range for incidence angles of ±20° from the boresight angle. The calibration was validated using other reference point targets: accuracy in σ^o value is within 2 dB, whereas the phase dispersion is within 5 degree [6]. The stability of the system calibration parameters was also assessed for various flights. The objective was to assess whether is it possible to calibrate one set of data using the calibration parameters of a previous flight, and the thermal noise measurement of the present flight. An offset of 3 dB in radiometry between the like and cross-polarization was noted. This is due to the fact that the like and the cross-polarized are fed to two different receivers, and that the thermal noise measurement does not include the amplifier device used to amplify the cross-polarized signal (generally much weaker than the co-polarized signal). The thermal noise measurements cannot account for phase shifts in the two separate receivers. This might lead to significant phase errors: 20° phase offset between the like and cross-polarization signal was noted for several flights [6]. Consequently, the system can be accurately calibrated provided that the reference targets were deployed during the flight (the system is stable during the same flight for various passes). For the scene under study, the pointing angle was of 58°, and the reference targets were deployed at about 60°. The scene was calibrated across the range 46° to 70°, and the calibration was validated using reference point targets (not used for the calibration).

III. Analysis of the ocean and ship polarization signatures

A. Ocean polarimetric signature

The co- and the cross-polarized signatures were analyzed across the scene incidence angle range 46°-70°. The results obtained are consistent with ones obtained in [9]. At the considered incidence angles, the Bragg scattering mechanisms dominates, and the co-polarized signatures exhibit a saddle point at horizontal polarization, and a maximum at vertical polarization which becomes more pronounced with increasing incidence angle. The cross-polarized signatures manifest a maximum at circular polarization (RL and LR) and a minimum at HV and VH polarizations. At 45°, the cross-polarized signature still remains the Rican signatures obtained at lower incidence angle. The difference between the HV polarization and the other linear polarization increases with incidence angle, confirming the Bragg scattering mechanisms at high incidence angles.

B. Ship polarimetric signature

The co- and cross-polarized signatures obtained for the ships illuminated over the scene have complex shapes. Few of them vaguely resemble the theoretical polarimetric signatures obtained for a conducting short thin cylinder in [8] with the maximum copolarized response and the minimum in the cross-polarized response occurring at the linear polarization with the same orientation as the cylinder. For few ships, the cross-polarized signature exhibit a minimum at HV, and a maximum around the circular polarization (RL). The maximum of the co-polarized signature occurs close to the horizontal polarization HH.

IV. Potential of the classical linear and circular polarization for ship detection

A. HH, VV, and HV polarization

At HV polarization the ocean signature is low as is the ship response, as noted in Section III. Analysis of the images shows that many ships are not detected in the HV polarization. More ships are missed with the VV polarization. HH gives the best results among the classical polarizations HV and VV. Unfortunately, the ship-sea contrast starts to be significant at incidence angles higher than 55°. At lower incidence angles, the ocean clutter is high which explains the low contrast (see figure 1 with incidence angle 46° to 68°). This result might be extended to lower incidence angles, and the polarization HH is only effective for incidence angles higher than 55°.

B. Circular polarization

At low incidence angles, the ocean backscattering is mainly dominated by specular scattering as shown in [9]. One might think that the ship backscattering is dominated by double bounce scattering mechanisms. The circularly polarized receiving antenna is matched to the transmitting one to minimize the single bounce backscattering, and to maximize the double bounce return. The ship-sea contrast looks better than the one obtained with HH polarization at the lowest scene incidence angles (45° to 55°). The results should be better at lower incidence angles. This will be confirmed in the next study using polarimetric data collected with a lower antenna pointing angle. At higher incidence angles, the ocean backscattering differs from the specular mechanism type, and the ship-sea contrast decreases.

V. Polarization entropy for ship detection

The analysis of ship and ocean polarization signature leads to the conclusion that the ship-sea contrast is not optimum if only one pair of transmitting-receiving antenna polarizations are used. Several algorithms have been developed for contrast enhancement (see for example [1]). Each pixel of the optimized image corresponds to a separate combination of transmitting-receiving polarizations. In this paper, the polarization entropy is defined as the polarization information content related to target nonstationarity. The higher the polarization entropy, the larger the signal variation with transmitting-receiving polarizations. Figure 2 shows the polarization entropy of the image under study. For low incidence angles up to 60 degrees, the Braggs ocean mechanism has a lower entropy compared to the ship's polarization entropy. The ships which can hardly be seen in the HH polarization (figure 1) are now well enhanced. This method should be very efficient for low incidence angle (20° to 60°°). At higher incidence angles, the ocean entropy becomes close to the ship one, and the polarization entropy can no longer discriminate ship from ocean. This should not limit the application of the method as most satellite SARs generally operate at incidence angles lower than 60°.

VI. Conclusion

Ship detection is a very complex problem which can hardly be optimized with conventional SARs which use only one polarization for transmission, and one polarization for reception. The polarization entropy looks to be very promising for ship detection at incidence angles lower than 60°. These results should promote the use of fully polarimetric data. The launch in the near future of Radarsat 2 which will have this unique capability would certainly make polarimetric data more accessible. Such potential can only be well exploited provided that Radarsat 2 polarimetric modes will be well calibrated.

In the future, other campaigns will be performed with the Convair-580 to validate this method at lower incidence angles (20° to 40°). Tests will be performed for different ships at various orientations, and at different wind conditions. A matched filter based on the polarization entropy is currently being developed at CCRS.

Acknowdlegments

The author would like to thank Dr. R.K. Hawkins from CCRS for helpful discussions and for organising the flights, and S. Nedelcu under contract with Intermap for having processed the data. The support of Environment Canada which now owns and operates the system is also acknowledged.

References

[1] W.M. Boerner, M. Walther, and A.C. Segal. Development of the polarimetric contrast enhancement optimization procedure and its application to sea surface scatter in POL-SAR image analysis. In *Proc. of IGARSS'93, Tokyo, Japan, August 18-21*, 1993.

[2] K. Eldhuset. An automatic ship and ship wake detection system for spaceborne SAR images in coastal regions. *IEEE Trans. Geoscience Rem. Sens.*, 34(4):1010–1019, 1996.

[3] R.K. Hawkins, P. Vachon, J. Cranton, and K. Murnaghan. Scene descriptions for CV-580 SAR acquisitions St Magaret's Bay area. In *Report CCRS-TN-1998-021*, 1998.

[4] C. E. Livingstone, A. L. Gray, R. K. Hawkins, P. W. Vachon, T. I. Lukowski, and M. LaLonde. The CCRS airborne SAR systems: Radar for remote sensing research. *Can. J. Rem. Sens.*, 21(4):468–491, 1995.

[5] R. Touzi, C. E. Livingstone, J. R. C. Lafontaine, and T. I. Lukowski. Consideration of antenna gain and phase patterns for calibration of polarimetric SAR data. *IEEE Trans. Geoscience Rem. Sens.*, 31(6):1132–1145, 1993.

[6] R. Touzi and S. Nedelcu. Calibration of the polarimetric Convair-580 C-band SAR. In *Report provided to the Defense Research Establishment of Ottawa (DREO) under the CCRS/DREO agreement FY97/98*, 1998.

[7] P. W. Vachon, J. W. M. Campbell, C. Bjerkelund, F. W. Dobson, and M. T. Rey. Ship detection by the RADARSAT SAR: Validation of detection model predictions. *Can. J. Rem. Sens.*, 23(1):48–59, March 1997.

[8] J.J. Van Zyl and F.T. Ulaby. Scattering matrix representation for simple targets. In F.T. Ulaby and C. Elachi, editors, *Radar Polarimetry for Geoscience Applications*, chapter 2, pages 17–50. The Artech House Remote Sensing Library, 1991.

[9] J.J. Van Zyl, H.A. Zebker, and C. Elachi. Imaging radar polarization signatures: theory and observation. *Radio Science*, 22:529–543, 1987.

Fig. 1. *HH image (46°-70°)*

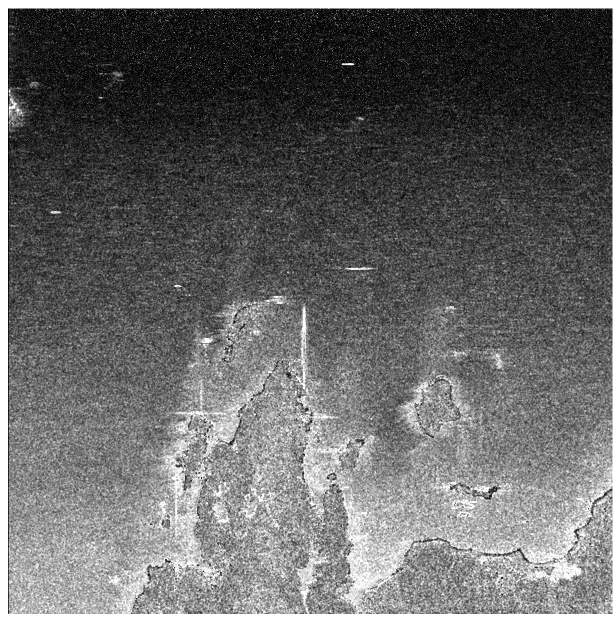

Fig. 2. *Polarization entropy image*